

Acoustic and photographic studies of injected bubbles

T G Leighton, K J Fagan and J E Field

Cavendish Laboratory, Madingley Road, Cambridge CB3 0HE, UK

Received 26 July 1990

Abstract. When gas bubbles are injected into a liquid, their behaviour can be markedly different from the single, isolated, spherical oscillating bubble, since shape oscillations can distort the bubble. In addition, the process of bubble formation can lead to multiple excitations of the bubble oscillations, for example when the newly formed bubble contacts and absorbs the bubble being formed at the nozzle. This gives rise to corresponding features in the acoustic output. In this study the photographic and acoustic data from such events are correlated. This undergraduate-level experiment provides useful data in a field of current interest.

Résumé. Quand des bulles de gaz sont injectées dans un liquide, leur comportement peut être nettement différent de celui d'une bulle isolée, sphérique, oscillante car des oscillations de forme de la bulle peuvent la déformer. De plus, le processus de formation de bulles peut donner lieu à des excitations multiples des oscillations de ces bulles, par exemple lorsque la nouvelle bulle qui vient d'être formée entre en contact et absorbe la bulle dans l'injecteur. Ceci donne lieu à des effets correspondants dans l'émission acoustique. Dans cette étude, les données photographiques et acoustiques de tels événements ont été corrélées. Cette expérience de niveau 'undergraduate' fournit des données utiles dans un domaine actuellement intéressant.

1. Introduction

The acoustic output from a freely oscillating bubble was first examined by Minnaert (1933), who showed that the sound emissions could be predicted from a simple model of a spherical bubble undergoing simple harmonic motion. For a bubble of equilibrium radius R_0 , oscillating under a static pressure P_0 in a liquid of density ρ , the natural frequency of spherical pulsation is

$$\nu = \left(\frac{1}{2\pi R_0} \right) \left(\frac{3KP_0}{\rho} \right)^{1/2} \quad (1)$$

where K is the so-called polytropic index, which takes values between unity and γ (the ratio of heat capacities at constant pressure and volume) depending on whether the gas behaves isothermally, adiabatically, or in some intermediate manner. Leighton and Walton (1987) confirmed this, and employed the correlation to determine the bubble populations in natural environments. Their initial experiment was simple, requiring only a hydrophone (or water-proofed tweeter) to monitor the acoustic emissions generated as single bubbles were injected into a water tank. However, photography of these bubbles showed that, although the acoustic emissions agree well with equation (1), these bubbles are far from the ideal case: the equilibrium shape is, of course, non-spherical as a

result of buoyancy forces; and shape oscillations can greatly distort the bubble.

The shape oscillations of gas bubbles in a liquid have been studied theoretically. Rayleigh (1879) used dimensional analysis of the analogous case of the shape oscillations of small drops, formed by the fragmentation of jets, to predict the frequency of shape oscillations. Lamb (1924) completed Rayleigh's analysis. Stokes (1868) argued that the radial component of the particle velocity around an oscillating sphere is proportional to $1/r$, whilst the lateral velocity component falls off as $1/r^2$. Therefore the acoustic emission from an oscillating bubble should be dominated by the spherically pulsating zero-order mode, and the shape oscillations should give rise to little acoustic emission. Analysis by Longuet-Higgins (1989a) showed that an asymmetric normal-mode oscillation generates monopole radiation at second order. Longuet-Higgins (1989b) theoretically analysed the subsequent behaviour of a bubble that has an initial distortion, but with no initial volume change. He showed that the initial distortion can be expressed as the sum of spherical harmonics, and that the subsequent motion can be resolved into the normal modes, each of which radiate independently at second order. The analysis predicted that the zero-order mode would be excited. Resonance between a given harmonic and the zero-order mode was shown to be

important. Beats set up between these can give rise to envelope modulation of the acoustic emission. Longuet-Higgins (1989b) was able to compare data for the shape oscillations with the photographic results of Fitzpatrick and Strasberg (1957), and concluded that such predictions would be of use in analysing naturally occurring sound in the oceans.

An understanding of the bubble-generated noise in the sea is currently the subject of much work, having many applications. Underwater communications employing ultrasonics is an obvious example, since the background noise that can degrade such signals must be understood. Similarly, since bubbles can be sized from their acoustic emissions (Leighton and Walton 1987), these studies are of potential value to a range of problems. Rainfall, for example, can produce oscillating bubbles (Pumphrey and Walton 1988, Pumphrey and Crum 1989) and such acoustic studies are applicable to weather sensing. Also, a knowledge of the bubble population in the sea can give information on the dissolution of atmospheric carbon dioxide from the atmosphere, and so has relevance to the 'greenhouse' effect: it is estimated that the oceans absorb one to two gigatonnes of carbon each year (Anderson and Bowler 1990).

Medwin and Beaky (1989) categorized the acoustic emissions from bubbles (both single and in clusters) into five groups. In the present work we identify and study a sixth emission type, quite distinct from the others, resulting from contact between bubbles. The basic experiment is relatively simple (potentially of undergraduate level) but enables the direct examination of both the shape oscillations and of the processes that excite acoustic emission.

2. Experiment

The apparatus (figure 1) is substantially similar to that described in Leighton and Walton (1987). A bubble is injected through a nozzle into the base of a tank of water. The pressure of the gas within the syringe can be manually altered by simply depressing the plunger with more force, so increasing the gas flow through the nozzle. A steel nozzle of internal diameter 0.5 mm, and external diameter 1.6 mm, was used. Single or trains of bubbles, with associated coalescence effects, could be produced depending on the chosen gas pressure. A hydrophone (Bruel and Kjaer type 8103), placed so that the oscillating bubble is 10 mm from the active element and level with it, detects the acoustic emissions which are then recorded on a storage oscilloscope. High-speed photography was used to image the processes of bubble formation and shape oscillation, using a Hadland Hyspeed camera. It was not possible to record the sound simultaneously with the photograph, though conditions proved to be very reproducible.

For the undergraduate laboratory, simpler equip-

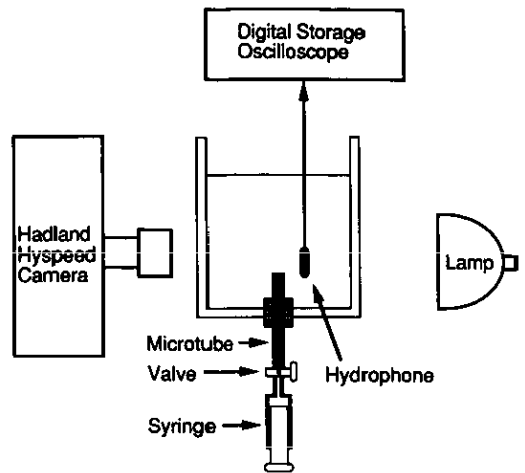


Figure 1. The apparatus used to record bubble production from nozzles. The hydrophone was removed for the photography.

ment could be used. As has been described in Leighton and Walton (1987) a waterproofed tweeter provides a useful and much cheaper alternative to a hydrophone. It is uncalibrated though linear in acoustic pressure, and is accurate for frequency information. Variably-delayed flash photography, triggered from the hydrophone output, can be used as an alternative to high-speed photography.

3. Results

Figure 2 shows a series of five frames from a high-speed film, showing an air bubble being blown from the metal nozzle (which is visible at the base of each frame). The initial shape distortion of the bubble, caused by the buoyancy and adhesion forces, results in subsequent shape oscillations. The first-order spherical harmonic dominates, the shape oscillating between having the long axis vertical (called, in the extreme, the 'needle' shape), and having it horizontal (the 'pancake' shape). The frames chosen show the limits of the oscillation: frames 2 and 12 have the long axis vertical; frames 7 and 17 have it horizontal. Buoyancy also tends to lengthen the horizontal axes, a feature which dominates the shape as the oscillations dampen out. Such photographic data are suitable for comparison with results from the numerical techniques of Longuet-Higgins (1989b). The acoustic output of such a bubble is shown in figure 3(a).

If, however, the air flow through the nozzle is increased, bubble production becomes more complex (figure 4). The result is not simply an increased rate of generation of bubbles of the same size as those seen in figure 2, with the bubbles undergoing mainly first-order shape oscillations that are the result of their initial shape. Instead, a rising bubble (for example, the

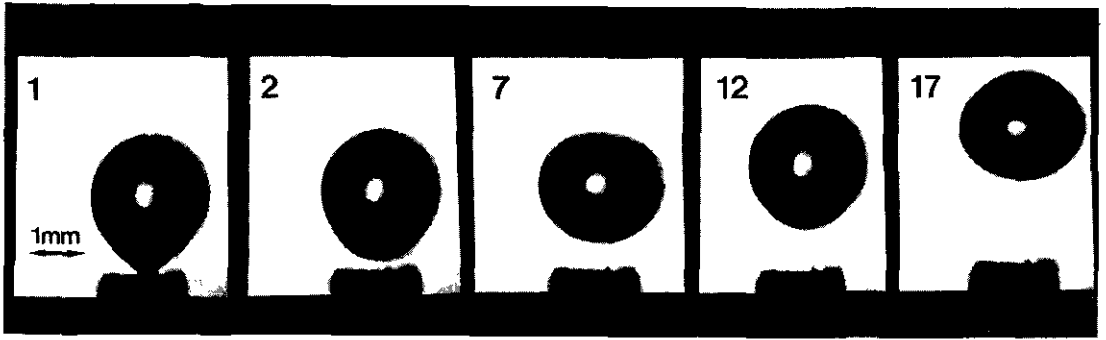
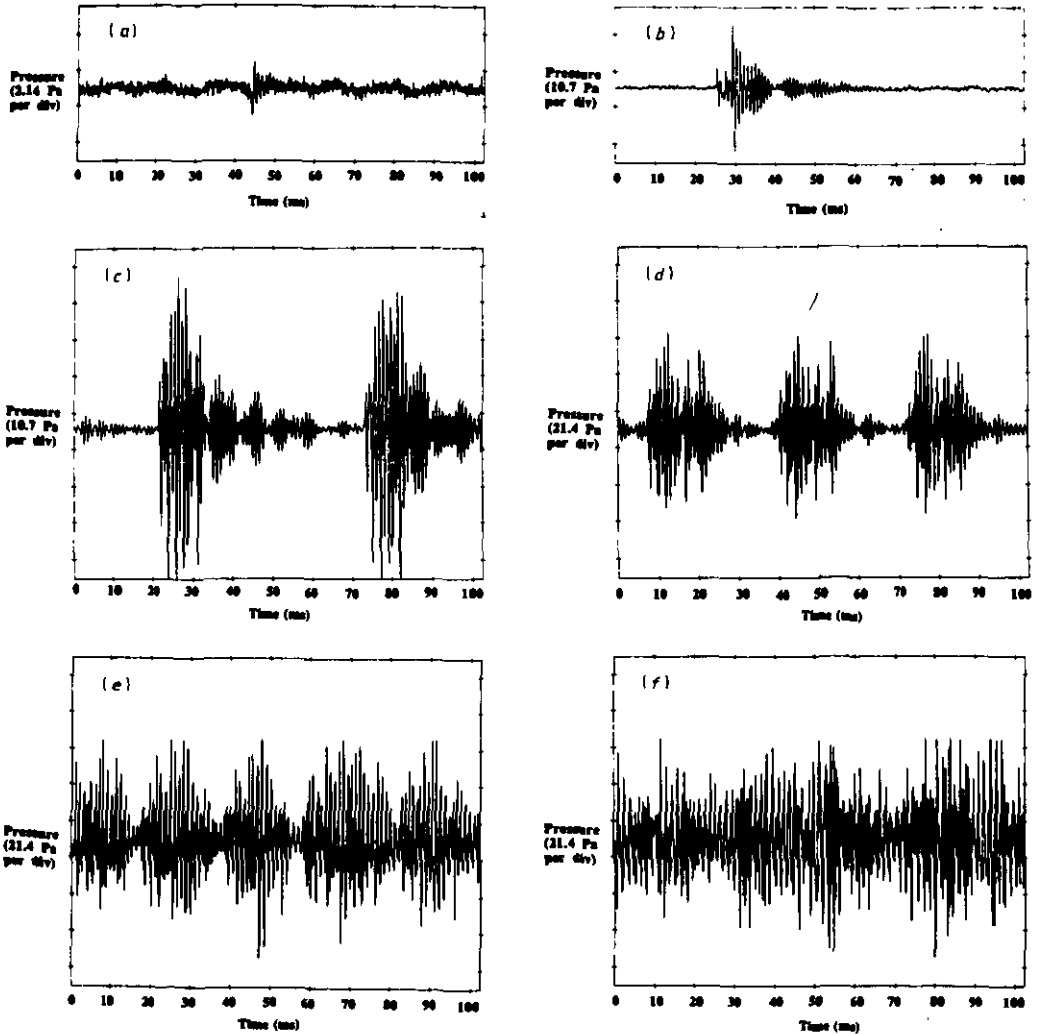


Figure 2. Selected frames from a high-speed photographic sequence, showing a bubble released from a metal nozzle. Inter-frame time 0.71 ms.

Figure 3. The acoustic readings for the release of bubbles from the metal nozzle. Figure 3(a) is for the release of a single bubble. The recordings are for increasing gas flows: (b) 0.1 ml s^{-1} ; (c) 0.2 ml s^{-1} ; (d) 10 ml s^{-1} ; (e) 15 ml s^{-1} ; (f) 30 ml s^{-1} .



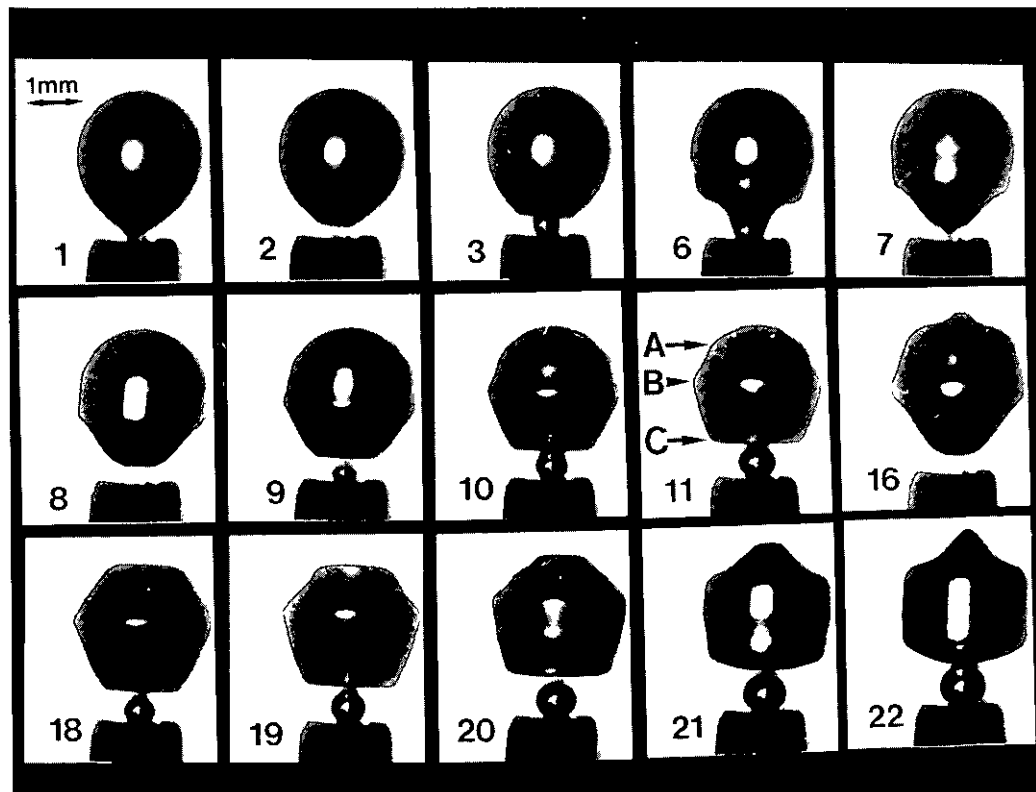
one which detached from the nozzle in frame 2) is contacted by its successor, which is growing at the nozzle (frame 3). This contact causes further shape oscillation in the initial bubble. The two bubbles merge, the successor detaching from the nozzle (frame 7). Both merging and detachment cause further shape oscillations, which have the appearance on the film of ripples on the bubble surface, progressing up the bubble. These ripples, after reaching the bubble top, travel down the bubble wall. Three ripples can be seen in frame 11. Ripple A was stimulated by the detachment shown in frame 2. Ripple B was the result of contact of the main bubble with its successor (seen in frame 3). This ripple is particularly pronounced since coalescence of the main bubble with the successor distorts the bubble wall behind it into a concave shape (frame 6). Ripple C was excited by the detachment shown in frame 8. Ripple A reaches the top of the bubble in frame 16, and then travels down, to interfere with ripple B (travelling upwards) in frame 18. Of course, these ripples are merely expressions of shape oscillations that could be expressed in terms of spherical harmonics.

These processes continue, with the main bubble absorbing several successors, and each time its volume is increased. Subsequent to these frames, the

main bubble touches its successor without coalescence: such contact can excite shape oscillation. The main bubble then rises out of the proximity of the nozzle, and the bubbles growing there. In total, four successors were absorbed.

The processes shown in figure 4 can drastically influence the acoustic output of bubbles blown from nozzles. The volume of the main bubble increases with each contact, which reduces the frequency of the sound (see equation (1)). However, each contact, as well as exciting shape oscillations, excites the zero-order 'breathing' mode, and so the acoustic output takes the form as seen in figure 3(b). With each contact, the acoustic output is excited afresh. On the film from which figure 4 is taken, these contacts occur every seven to ten frames (the interval increasing in time), corresponding from 1.68 to 2.40 ms respectively. By comparing this time with figure 3(b), it can readily be seen that several of these excitations occur before the first minima in the envelope. Therefore it follows that here these inter-bubble contacts are responsible for increasing the magnitude of the acoustic emission above that expected from a single bubble simply released from a nozzle (the acoustic pressure amplitudes in figure 3(b) are about ten times those seen in figure 3(a)). The initial excitation, caused by the

Figure 4. Selected frames showing a bubble released from a metal nozzle being excited by contact with, and absorption of, successors growing at the nozzle. Inter-frame time 0.24 ms. Gas flow $\approx 0.1 \text{ ml s}^{-1}$.



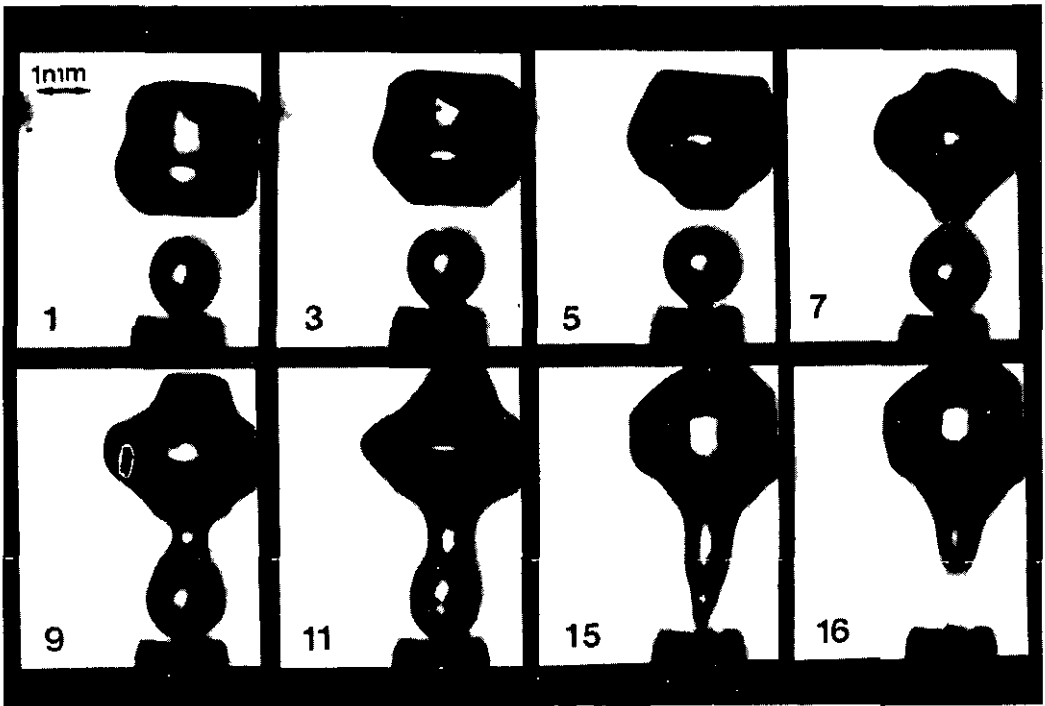


Figure 5. Selected frames showing a bubble released from a metal nozzle being excited by contact with, and absorption of, successors growing at the nozzle. Inter-frame time 0.22 ms. Gas flow ≈ 0.2 ml s^{-1} .

release, is of smaller amplitude than those caused subsequently by inter-bubble contact. The modulations in the envelope have a period of order 10 ms, frequency ≈ 100 Hz (corresponding to about 40 frames in figures 4 and 5). This is likely to be a result of beat frequencies between modes, as discussed by Longuet-Higgins (1989b).

If the gas flow through the nozzle is further increased, the rate of growth of the successors is increased. This means that more successors can be absorbed. Figure 5 illustrates such a case, showing the final contact of the main bubble with those at the nozzle. This bubble absorbed in total five successors. The main bubble is more frequently excited by these contacts than it was at the lower gas pressure, and its final volume is larger. Thus the departures from sphericity are more pronounced. This, coupled with the fact that the successors grow more rapidly, means that even when the main bubble is far from the nozzle (see, for example, frame 1, which was taken 13.7 ms after the initial release of the bubble), a pronounced shape oscillation (frame 7) can lead to absorption of the successor (frame 16). The increased number of contacts is reflected in the increased amplitude in the acoustic signal seen from figure 3(b, c).

The shape seen in frames 7 to 15 of figure 5 becomes the characteristic form as the air flow through the nozzle is increased.

As the gas flow increases further, the successor grows more rapidly, and is absorbed by the main bubble series without detachment from the nozzle (figure 6). In this way, gas is pumped directly into the large bubble complex. These processes are clearly visible in figure 6. The bubble complex here consists of three joined bubbles (labelled in frame 1). The successor, bubble C, grows, whilst the intermediate bubble (B) elongates as a result of shape oscillations and buoyancy forces. At some point, the angle of contact between the bubble walls of C and B goes from less than to greater than 90° (this occurs between frames 5 and 6) and bubble C is then absorbed by bubble B. However the next successor (labelled D) is growing at the nozzle tip, and is attached to bubble C. The process then repeats, and so gas is pumped directly from the nozzle into the intermediate bubble. If the intermediate bubble is joined to the superior, gas can be pumped directly into the latter. After a time, the increasing size of the superior bubble (A) causes it to separate from the intermediate bubble, when the increasing buoyant forces on A produce detachment. Shape oscillations may narrow and weaken the contact point between superior and intermediate.

As the gas flow increases, the size of the main components of the bubble complex increases. Surface tension forces are therefore less able to maintain sphericity (for example, in the intermediate bubble in

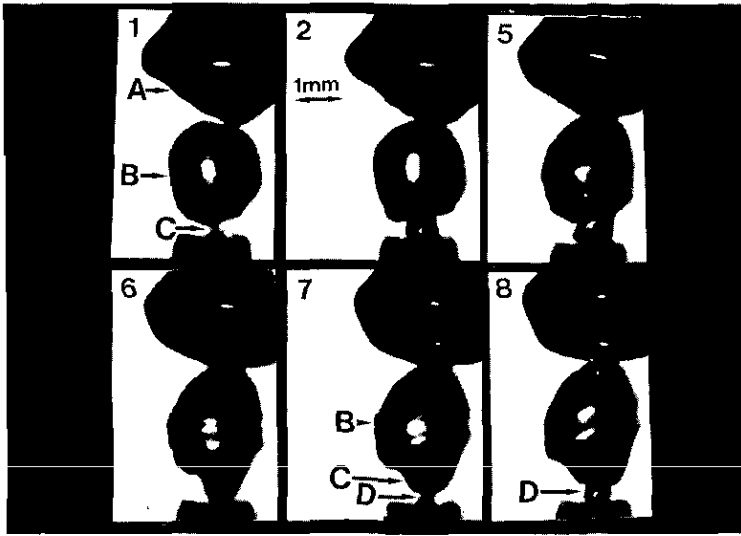


Figure 6. Selected frames showing the characteristic form of gas flow from the nozzle. Inter-frame time 0.17 ms. Gas flow $\approx 5 \text{ ml s}^{-1}$.

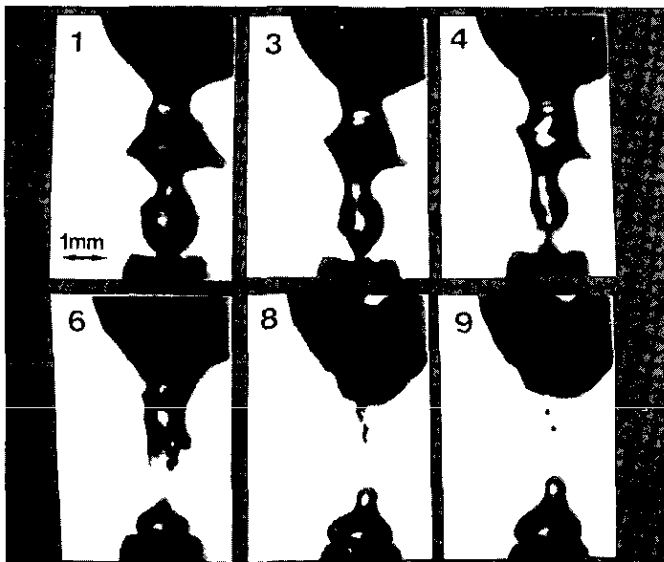
figure 7), and fragmentation can be seen (frames 8 and 9). The production of such small bubbles contributes to high-frequency acoustic emissions, of the sort seen in figure 3(*d-f*).

Figure 8 shows the bubbles at higher gas flow rates. The superior (labelled A) is large, and absorbs the intermediate bubble (labelled B) in frames 1 to 3. The successor grows to replace the intermediate bubble (bubble C in frames 1 to 8), and is itself replaced by bubble D. Gas is pumped through the successor

bubbles into the superior bubble. Again, the detachment of fragments (labelled E) from the superior bubble contributes both to the observable bubble flow to the liquid surface, and to the sound emission.

In addition to these rising fragments, larger bubbles can eventually be detached from the complex through the action of shape oscillations in the superior. This is happening regularly in the process shown in figure 9. The perturbation which results from the absorption by the superior bubble A of the intermediate bubble

Figure 7. Selected frames showing the characteristic form of gas flow from the nozzle. Fragmentation occurs. Inter-frame time 0.16 ms. Gas flow $\approx 10 \text{ ml s}^{-1}$.



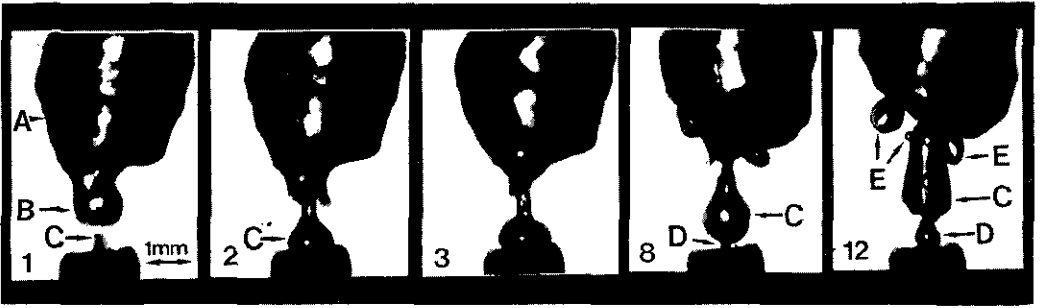


Figure 8. Selected frames showing the characteristic form of gas flow from the nozzle. The three-bubble system is clearly visible: superior, A; intermediate, B; successor, C. Fragmentation occurs. Inter-frame time 0.24 ms. Gas flow $\approx 15 \text{ ml s}^{-1}$.

B in frame 10 excites a shape oscillation which tends, in frames 16 to 40, to divide the superior in two. It is the culmination of such a cyclic process which, in frame 6, causes the separation of a large bubble (labelled S) from the top of the superior.

At the highest injectable flow rates in this experiment the acoustic signal is complex (figure 3(f)), characterizing a system where there is little uniformity in the size of the bubbles produced.

Experiments from a variety of other nozzles show similar general behaviour. The size of the nozzle affects the size of bubble produced, and therefore the magnitude of the shape oscillations and the growth rate of the successors. The nature of the nozzle and liquid will affect their adhesion, and therefore determine whether the successor tends to detach from the nozzle and so be absorbed by the main bubble, or whether it remains attached to the nozzle and merely touches the main bubble.

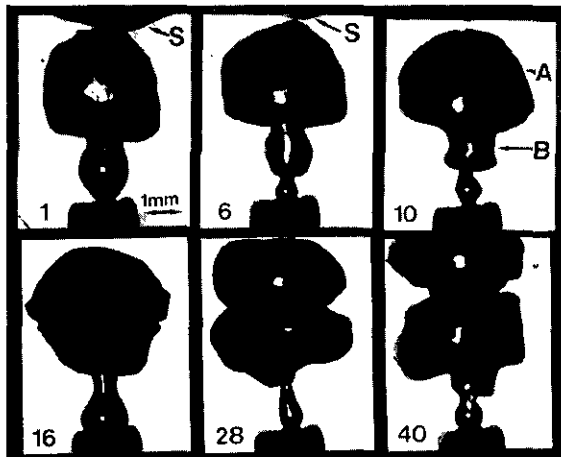
A drawn glass nozzle, which generated bubbles of radius $0.87 \pm 0.06 \text{ mm}$, produced the acoustic out-

put shown in figure 10. Multiple excitations can clearly be seen, and photography proved this to be the result of contact between, and coalescence of, the released bubble and the successors. The decay of these oscillations is more rapid than that of the bubble system of figure 3 (owing to the smaller size of bubbles produced), so that each excitation is visible as a separate pulse. In figure 10(a) there is one inter-bubble contact following detachment. The second excitation, due to this contact, is of higher amplitude than the primary, generated by the initial detachment of the bubble from the nozzle. Figure 10(b) demonstrates excitations resulting from many inter-bubble contacts.

4. Discussion

Despite pronounced shape oscillations, the acoustic output of a freely oscillating single bubble is dominated in the far-field by frequencies typical of the

Figure 9. Selected frames showing the characteristic form of gas flow from the nozzle. The three-bubble system is clearly visible. Inter-frame time 0.15 ms. Gas flow $\approx 30 \text{ ml s}^{-1}$.



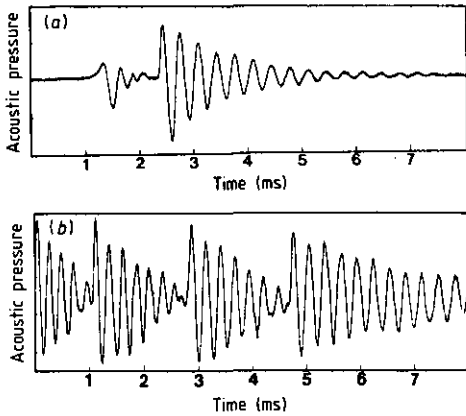


Figure 10. The acoustic trace from a glass nozzle of internal diameter 0.12 mm. Multiple excitations are seen. These are a result of the newly-released bubble absorbing its successor. The excitations are (a) larger than, or (b) of the order of the primary excitation.

simple spherical resonance calculated by Minnaert (1933), and as predicted by the theoretical arguments of Longuet-Higgins (1989b), where the breathing mode can be excited by resonance with the higher modes. It should be remembered that the experimental conditions described here are identical to those used by Leighton and Walton (1987), who used the experiment to confirm equation (1).

In many practical situations, shape oscillation in freely-oscillating bubbles can be the result of inter-bubble contact. These bubbles may already be oscillating. This source of shape-oscillation excitation is in addition to the type of situation discussed by Longuet-Higgins (1989b), where the bubble has an initial shape distortion with no volume change.

The acoustic output of freely-oscillating bubbles can be excited by inter-bubble contact. This can lead to a type of emission (see figure 10) in addition to those illustrated by Medwin and Beaky (1989). If the inter-contact time is short compared with the decay time, then such contacts produce overlapping excitations, increasing the overall amplitude of the acoustic output (figure 3).

There are several factors affecting the shape of a system of bubbles. Excited shape oscillations occur, and can in addition give the bubble a tendency to fragment (see, for example, figure 7 frame 9) or coalesce (for example, in figure 5 frame 7). In an attempt to minimize surface energy, two bubbles which have joined (with no intermediate septa) will tend towards sphericity. This is the cause of the absorption of bubbles seen, for example, in figure 4 frames 3 to 7, characterized by the angle of wall contact going from less than, to greater than, 90° . However, the pumping of gas into a bubble acts against this tendency; thus the successor at the nozzle will initially grow as an individual entity (figure 4

frames 9 to 11), before later coalescing with the intermediate bubble.

5. Conclusions

Inter-bubble contact can occur in several ways. Least intimate is a mere proximity effect, where one bubble can be thought of as being affected by the sound field or pressure gradients or fluid motions generated by another.

Alternatively, the bubbles might touch, and for some time the bubbles will share a septum that is a common region of bubble wall. The bubbles might then separate, or a closer contact might occur in which the septum breaks down, so that there is no physical barrier preventing the mixture of the contents of the two bubbles. From this situation, the bubbles might coalesce into a single bubble to minimize surface energy; alternatively surface modes, or the growth of one bubble through an injection of gas, may prevent the bubbles merging into one sphere. The bubbles may separate.

These processes can occur when bubbles are produced from nozzles. Such events can excite modes of oscillation in the bubbles. Other modes (such as the zero-order breathing mode) can also be excited through resonance with these higher modes.

This study has investigated the acoustic output of bubbles injected from nozzles. The frequency associated with the 'breathing' mode is detected, multiply excited by subsequent bubble contacts which stimulate shape oscillations (that is, higher modes). At higher gas flow rates, fragmentation generates smaller bubbles and so gives rise to high-frequency sound. High-speed photography showed these processes in detail and allowed a more complete explanation of the detected acoustic signals.

Acknowledgments

TGL wishes to thank Magdalene College, Cambridge, and the SERC for Research Fellowships. The authors wish to acknowledge the help of Mr C W H Beton in measuring the gas flow rates.

References

- Anderson I and Bowler S 1990 *New Scientist* **1707** 24
- Fitzpatrick H M and Strasberg M 1957 *Proc. 1st Symp. on Naval Hydrodynamics*, NAS-NRC Publ. 515 (Washington, DC: Washington Government Printing Office) pp 241-80
- Lamb 1924 *Hydrodynamics* 5th edn (Cambridge: Cambridge University Press) pp 448-50
- Leighton T G and Walton A J 1987 *Eur. J. Phys.* **8** 98-104

- Longuet-Higgins M S 1989a, *J. Fluid Mech.* **201** 525-41
— 1989b *J. Fluid Mech.* **201** 543-65
Medwin H and Beaky M M 1989 *J. Acoust. Soc. Am.* **86**
1124-30
Minnaert M M 1933 *Phil. Mag.* **16** 235-48
Pumphrey H C and Crum L A 1989 *J. Acoust. Soc. Am.*
85 1518-26
Pumphrey H C and Walton A J 1988 *Eur. J. Phys.* **9** 225-
31
Rayleigh 1879 *Proc. R. Soc.* **29** 71-97
Stokes 1868 *Trans. Cambridge Phil. Soc.* **4** 299-317